

## Investigation of Lower Hybrid Wave Linear Conversion in FT-1 Tokamak by RADAR Enhanced Scattering Diagnostics

D.G. Bulyiginskiy, A.D. Gurchenko, E.Z. Gusakov, V.V. Korkin,  
M. M. Larionov, K.M. Novik, Yu.V. Petrov, A.Yu. Popov,  
V.L Selenin, A.Yu. Stepanov

*Ioffe Physico-Technical Institute,  
Politehnicheskaya 26, 194021 St. Petersburg, Russia*

The slow wave linear conversion in the Lower Hybrid Resonance (LHR) was proposed as a promising mechanism of ion heating in a tokamak plasmas in beginning of 70<sup>th</sup>. Since that time the investigations of this method were performed at different machines, utilizing different frequencies in the range from 300MHz to 2.5GHz [1]. In spite of numerous attempts, the role of the LHR in the slow wave absorption was not clearly demonstrated and effective ion heating was not achieved. Evidences of a rather complicated picture of LH wave interaction with plasma, including nonlinear phenomena, was found instead, appealing for development of new sensitive methods of plasma wave diagnostics in a hot tokamak plasmas. Such a new diagnostic technique, utilizing the signal back scattered by density perturbations in the vicinity of the Upper Hybrid Resonance (UHR) of the probing microwave, so called Enhanced Scattering (ES) was proposed in 80<sup>th</sup> [2], to deal with this challenge. This diagnostics possess a merit of higher sensitivity due to electric field growth in the UHR and fine spatial resolution. The position of the scattering point is determined in ES by the UHR position, given by condition

$$\omega_i^2 = \omega_{ce}^2(x) + \omega_{pe}^2(x) \quad (1).$$

The spatial scan is performed by variation of incident frequency or magnetic field where as the wave number resolution is achieved by application of time resolved measurements, based on the effect of the scattering signal time delay in the UHR [3]. The relation between the ES signal time delay and the density perturbation wave number, reading as

$$t_d = \frac{2q\omega_i}{\left| \frac{\partial \omega_{pe}^2}{\partial x} + \frac{\partial \omega_{ce}^2}{\partial x} \right|} \quad (2),$$

was checked in numerous experiments in laboratory plasmas [3]. The first results of the application of RADAR ES diagnostics to study of LH waves propagation in FT-1 tokamak were published recently in [4]. A more detailed description of these experiments, carried out at different plasma densities and RF powers is given in the present paper.

The experiments were carried out at the FT-1 tokamak ( $R=62.5$  cm,  $a=15$  cm,  $B_t=1$  T,  $I_p=30$  kA,  $T_e=400$ eV) in discharges with two density levels  $n_e(0)=0.7 \times 10^{13}$  cm<sup>-3</sup> and  $n_e(0)=$

$1.1 \times 10^{13} \text{ cm}^{-3}$ , referenced below as low and high density discharge. The LH wave at frequency 360 MHz was excited in plasma by a loop antenna. The experiment was performed at two power levels 22 and 50kW. The microwave probing at frequency 27.6 GHz and power 50 W was performed both in the cross-section of LH antenna and opposite to it. (These cross-sections are mentioned below as LH and ES.) The X-mode emitting and receiving horn antennae were positioned in the equatorial plane at high magnetic field side of the torus. The amplitude modulation of the incident wave at frequency 10 MHz was used to get the time of flight resolved data. The AM phase delay measurement scheme was discussed in detail in [4]. The time delay of the scattered signal was determined using the value of the phase shift of its modulation in respect to the incident wave. Dependencies of the frequency spectrum, power and time delay of the ES signal in the 60 MHz band on the toroidal magnetic field were studied in the experiment for both the down and up shifted spectrum components, corresponding to LH waves propagating correspondingly into and outside the plasma.

These dependencies, measured in the ES cross-section are shown in Fig.1a,b for the case of

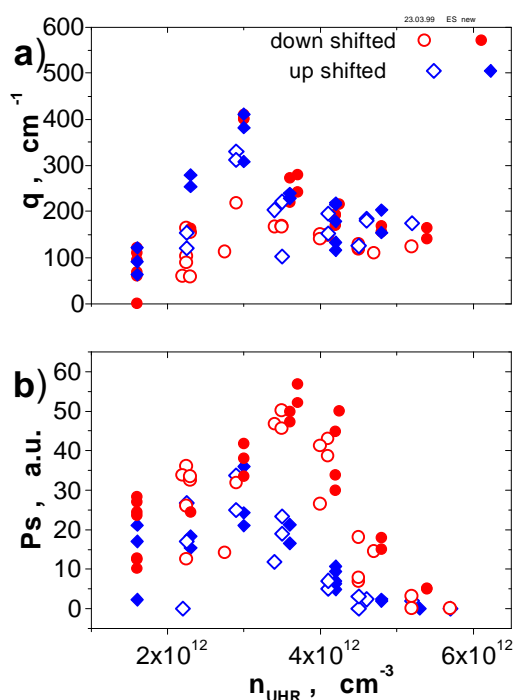


**Fig. 1** LH wave number (a) and ES power (b) in the ES cross-section versus  $n_{UH}$  ( $P_{LH}=22\text{kW}$ ,  $n_e(0)=7 \cdot 10^{12} \text{ cm}^{-3}$ ). Open and dark symbols correspond to beginning and end of RF pulse.

low density and low LH power. The magnetic field is expressed there in terms of  $n_{UH}$ , using (1). As it is seen in Fig.1a, the LH perturbation radial wave number increases with increasing  $n_{UH}$  for both spectral components. At  $n_{UH}=3 \times 10^{13} \text{ cm}^{-3}$  the wave number is maximal  $q=400 \text{ cm}^{-1}$  and then decreases to the level  $q=150 \text{ cm}^{-1}$  when  $n_{UH}=5.5 \times 10^{13} \text{ cm}^{-3}$ . At low densities  $n_{UH} < 3 \times 10^{13} \text{ cm}^{-3}$  the ES power is also comparable for up and down shifted components. However at larger UH densities, as it is shown in Fig.1b, the down shifted component dominates and, thus, the power of the wave propagating inside the plasma is a factor of 3 higher. The 3MHz wide LH line, shifted by 360MHz, is dominant in the spectrum under these conditions (see Fig.2a). The high values of wave number, observed in the experiment, could not be attributed to LH wave

and are only possible for Ion Bernstein Waves (IBW). To explain the above observations one could suppose that at  $n_{UH} > 3 \times 10^{12} \text{ cm}^{-3}$  ( $H < 10 \text{ kGs}$ ) the UHR is situated in the region of energy inflow, close to the LH resonance layer. Whereas at lower  $n_{UH}$  (higher magnetic fields) ES takes place far from the LH power stream.

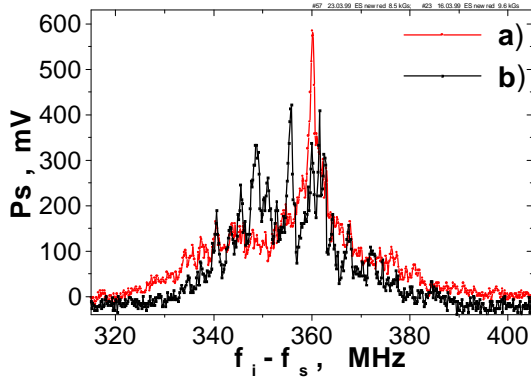


**Fig. 2** ES spectrum down-shifted component  
 a)  $P_{LH}=22kW$ ,  $n_e(0)=7 \cdot 10^{12}cm^{-3}$ ,  $B_0=8.5kGs$ ;  
 b)  $P_{LH}=50kW$ ,  $n_e(0)=1.1 \cdot 10^{13}cm^{-3}$ ,  $B_0=9.6kGs$

In order to check this supposition the dispersion curves of IBW and probing X-mode were analyzed in 1D geometry, only valid after linear wave conversion in the LHR. These curves are shown in Fig.3 by red lines for IBW and by green for the difference of incident and scattered wave number  $k_I - k_S$ . As it is seen in Fig.3a at  $H=9.5kGs$ ,  $n_{UH}=3.5 \cdot 10^{12}cm^{-3}$  the Bragg resonance conditions for ES –  $q = k_I - k_S$  is fulfilled at  $q=400cm^{-1}$ . At smaller magnetic field  $H=8kGs$ ,  $n_{UH}=4.7 \cdot 10^{12}cm^{-3}$  the Bragg resonance conditions could be fulfilled only at  $q=150cm^{-1}$ . Both values are close to the observed in Fig.1b, but

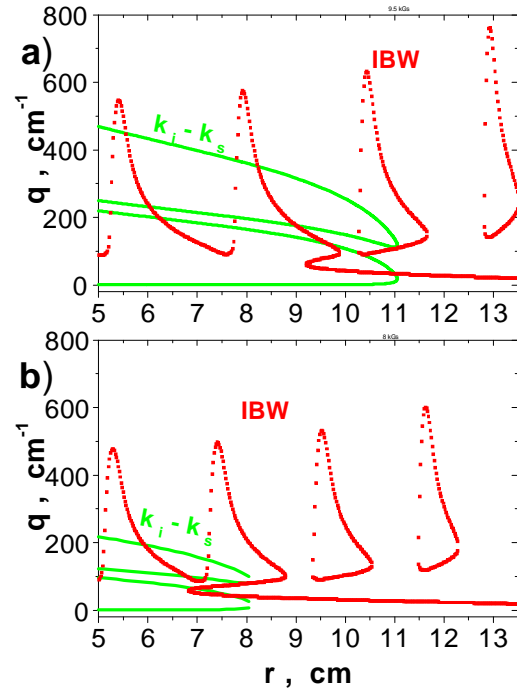


**Fig. 3** Dispersion curves for LH waves and probing waves ( $k_i - k_s$ ). **a)**  $B=9.5kGs$ ; **b)**  $B=8kGs$

nevertheless it is necessary to check if the linear conversion could take place in the ES cross-section at  $H \approx 9.5kGs$ . The  $\phi\theta$  projections of the LH wave ray trajectories, calculated at different magnetic fields, confirming this possibility are shown in Fig.4. The ray trajectories are started in the LH antenna cross-section with initial value of parallel refractive index  $N_{//}=7$  and finished after wave absorption in the LHR. According to [5], the value of  $z_{eff}=1.8$ , which is lower than typical for FT-1, was used in the ray tracing for this low density discharge. The distributions of  $q(n_{UH})$  and  $p_s(n_{UH})$ , measured in the same discharge in the LH cross-section are shown in Fig.5a,b. The wave number distributions, seen there are similar to those shown in Fig.1a, where as the ES power behavior is different. It increases, when the UHR is approaching the LH antenna, possess a minimum at  $n_{UH}=3 \cdot 10^{12}cm^{-3}$  and then increases till

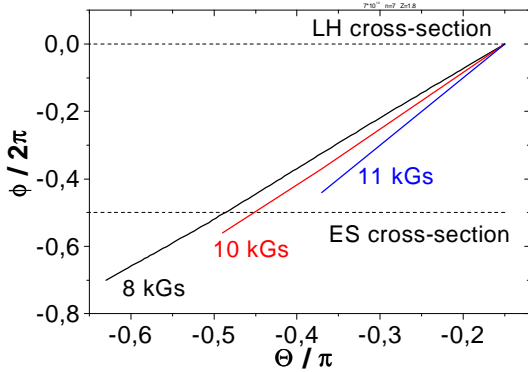


**Fig. 4** LH wave ray trajectories in the  $\phi\theta$  plane  
 $n_e(0)=1.1 \cdot 10^{13}cm^{-3}$

than typical for FT-1, was used in the ray tracing for this low density discharge. The distributions of  $q(n_{UH})$  and  $p_s(n_{UH})$ , measured in the same discharge in the LH cross-section are shown in Fig.5a,b. The wave number distributions, seen there are similar to those shown in Fig.1a, where as the ES power behavior is different. It increases, when the UHR is approaching the LH antenna, possess a minimum at  $n_{UH}=3 \cdot 10^{12}cm^{-3}$  and then increases till

the highest  $n_{UH}$  available in the experiment. Unlike Fig.1b, down and up-shifted satellites are comparable there and no maximum exists in the dependencies. This observation is in qualitative agreement with the ray tracing prediction, that for  $H>8kGs$  majority of ray trajectories reach the LHR before the LH cross-section and only at  $H<8kGs$ , at lowest magnetic fields, where ES is possible, the linear conversion takes place in this cross-section.

In the higher density discharge and at higher power the observed ES spectrum is much

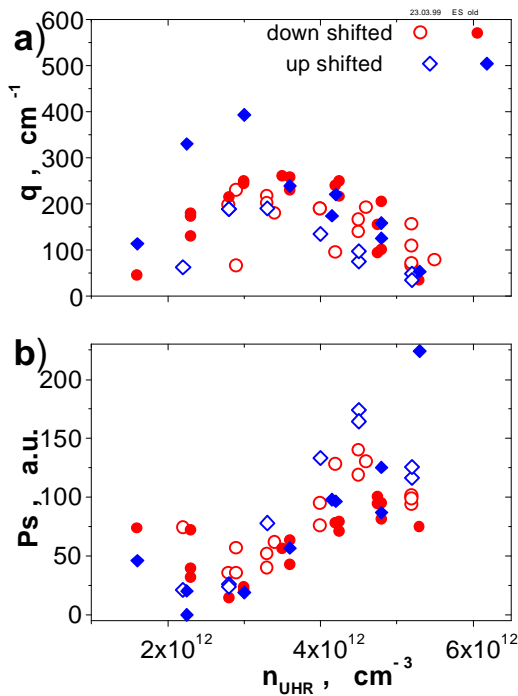


**Fig. 5** LH wave number (a) and ES power (b) in the LH cross-section versus  $n_{UHR}$  ( $P_{LH}=22kW$ ,  $n_e(0)=7 \cdot 10^{12}cm^{-3}$ )

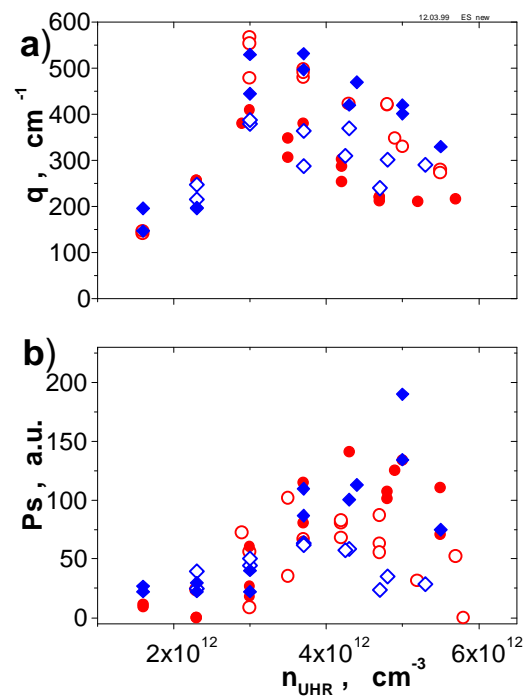


**Fig. 6** LH wave number (a) and ES power (b) in the ES cross-section versus  $n_{UHR}$  ( $P_{LH}=50kW$ ,  $n_e(0)=8 \cdot 10^{12}cm^{-3}$ )

broader (see Fig.2b), no exact LH line is observed. The wave numbers measured in the ES cross-section in low density discharge at 50kW of LH power are plotted in Fig.6a. The observed  $q$  values are much higher than at 22kW. They are increasing from the beginning of the RF pulse to its end following the growth of the plasma density from  $n_e(0)=0.8 \times 10^{13}cm^{-3}$  to  $n_e(0)=1.2 \times 10^{13}cm^{-3}$ . The ES power distribution shown in Fig.6b is similar for both spectrum components. The ES signal also increases from the beginning of the pulse to its end for both up and down-shifted components. The observed peculiarities of the ES signal behavior are most likely related to the nonlinear effects, which became more pronounced at higher density and LH power.

## References.

1. Golant V.E., Fedorov V.I. RF Plasma Heating in Toroidal Devices. Consultants Bureau New York.
2. Novik K.M., Piliya A.D. Plasma Phys. Control. Fusion, 1994, 36, 357.
3. Arkhipenko V.I., Budnikov V.N., Gusakov E.Z. et al. Plasma Phys. Control. Fusion, 1995, 37, A347.
4. Bulyiginskiy D.G. et. al. Proc. 25<sup>th</sup> EPS Conf. Contr. Fusion and Plasma Phys. 1998, V.22C, 1542.
5. Lashkul S.I. et. al. Sov. Journ. Appl. Spectroscopy, 1991, 54, 887.